

Aperture Synthesis Shows Perceptual Integration of Geometrical Form Across Saccades

Perception

1–15

© The Author(s) 2017

Reprints and permissions:

sagepub.co.uk/journalsPermissions.nav

DOI: 10.1177/0301006617739804

journals.sagepub.com/home/pec



Kai Schreiber

Max-Planck Institute for Metabolism Research, Cologne, Germany

Michael Morgan

Division of Optometry, City University of London, UK

Abstract

We investigated the perceptual bias in perceived relative lengths in the Brentano version of the Müller-Lyer arrowheads figure. The magnitude of the bias was measured both under normal whole-figure viewing condition and under an aperture viewing condition, where participants moved their gaze around the figure but could see only one arrowhead at a time through a Gaussian-weighted contrast window. The extent of the perceptual bias was similar under the two conditions. The stimuli were presented on a CRT in a light-proof room with room-lights off, but visual context was provided by a rectangular frame surrounding the figure. The frame was either stationary with respect to the figure or moved in such a manner that the bias would be counteracted if the observer were locating features with respect to the frame. Biases were reduced in the latter condition. We conclude that integration occurs over saccades, but largely in an external visual framework, rather than in a body-centered frame using an extraretinal signal.

Keywords

eye movements, imagery, object recognition, tracking/shifting attention

Introduction

When normal healthy observers scan a scene by moving their eyes, they usually experience a stable, spatially extended world, despite the rapid overlay of images from different parts of the scene on the retina. If the same sequence of images is presented to the retina with the eyes stationary, with the same temporal structure, the result is bewildering rather than informative. However, this result does not mean that eye position is taken into account when perceiving the world during normal eye movements. The alternative explanation is that we normally see only one image per fixation, the previous images being abolished by

Corresponding author:

Michael Morgan, Division of Optometry, City University of London, UK.

Email: m.morgan@city.ac.uk

backward masking and saccadic suppression. It could be the absence of saccadic suppression in the eyes-stationary condition that makes the rapid sequence hard to interpret. Experimental studies of “change blindness” with the eyes stationary support the idea that there is in fact rather little perceptual synthesis over successively presented images and that such as occurs is at a symbolic cognitive level rather than the building up of a jigsaw from fragments. For example, studying the limitations of change detection in multiple Gabor targets, Wright, Green, and Baker (2000) showed severe limitations even with as few as four elements.

The extent of integration across eye movements has been studied by several methods. All of them prevent the observer from seeing the figure as a whole, but require perception of the whole figure to be built up over time from fragments. In an early study of this type, Rock and Halper (1969) had participants track a spot moving around the outline of an invisible 2-D shape in a darkened room or to fixate a stationary spot and note the shape described by a moving spot. There was no difference between the two conditions, showing that an extended retinal image was not required. However, if observers tracked a moving spot and had to describe the retinal path taken by a stationary dot, performance was poor. Rock and Halper conclude that an extraretinal signal can be used to construct a form without an extended retinal image. However, the room in which the experiment took place was described as merely “darkened” or “room lights off,” so the possibility exists that dim background features existed, with reference to which the shape could be constructed without extraretinal information. The possible importance of background was indicated in a second experiment, where participants tracked a narrow slit moving over an object; they were better at reporting the shape of the object with room lights on than with room lights off.

Rock and Halper’s experiments were conducted using smooth eye pursuit to reveal the hidden object. More relevant to saccades is the technique described by Hayhoe, Lachter, and Feldman (1991) in which participants were presented with three dots in succession, defining a triangle, and were required to report whether the top angle was acute or obtuse. The three dots were presented either simultaneously or with a range of inter-dot intervals. At longer intervals, observers were instructed either to fixate on a stationary dot within the notional triangle or to move their eyes between dot presentations to the approximate anticipated position of the next dot, thus ensuring that all dots fell roughly on the fovea. In the latter case, the stationary fixation point was either present or absent. Results showed little difference between the eyes-fixated and eyes-moving conditions when a stationary reference dot was present, but all four observers did worse when the stationary reference was removed.

Another method for studying form perception without an extended retinal image of the object has been Plateau’s (1836) “anorthoscopic” stimulus in which a shape moves behind a narrow aperture, usually a vertical slit. There was originally discussion of whether or not the resulting perception of an extended object was due to ‘post-retinal storage’ or to “retinal painting” from tracking eye movements. However, Morgan, Findlay, and Watt (1982) used retinal stabilization to show that both effects can be involved. With very narrow apertures (4.5 arcmin) and fast movements (6 deg/s), tracking eye movements were necessary for veridical reports of shape width; while for wider apertures (9 arcmin) and slower movements (1.5 deg/s), they were not. The report by Parks of seeing a “camel through the eye of a needle” was thus almost certainly due to retinal painting. Morgan et al. (1982) used some quite complex figures, such as a rotating and translating spoked wheel; and the Brentano version of the Muller-Lyer figure. In the latter case, the normal bias of seeing the midpoint shifted toward the outgoing arrow was found, even without “retinal painting.” However, as Morgan et al. and subsequently Day and Duffy (1988) emphasized, the results

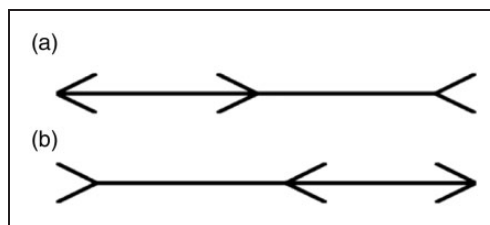


Figure 1. Brentano version of the Müller-Lyer illusion in leftward-pointing (a) and rightward-pointing (b) configuration.

do not necessarily demonstrate the construction of a spatially extended percept. One possibility is that participants base their decision of the time elapsing between appearance of the midpoint marker in the aperture, and the first appearance of the arrowhead, which will occur earlier for the ingoing than the outgoing arrow. Indeed, Day and Duffy (1988) showed that temporal judgments were influenced in exactly this manner.

Our present article combines the techniques of Hayhoe et al. (1991) and Morgan et al. (1982) by revealing a Brentano figure over successive fixations. The method is illustrated in Figures 1 and 2.

A stationary Brentano figure was constructed on a CRT, but only revealed in a Gaussian window centered at fixation. Participants were free to move their eyes around the figure to build up a “picture in the mind’s eye” of the underlying figure. On each trial, there were two “probe” presentations in succession, one above and one below the center of the screen, and participants were required to decide in which of the two probes the midpoint marker was nearer the actual midpoint. Both probes, the reference and the test, had the same pedestal offset from zero; in addition, the test had an additional offset chosen from a list without replacement. We used this two-alternative forced choice (2AFC) task (with roving pedestal) rather than the more commonly used Method of Single Stimuli (MSS) because of evidence that the latter is susceptible to cognitive manipulation (Mather & Sharman, 2015; Morgan, 2014; Morgan, Melmoth & Solomon, 2013). For example, using the MSS, participants could easily give the appearance of having a perceptual bias by preferentially pressing the button on the side the overall arrow points to, to indicate that the midpoint marker is nearer the pointed side of the figure.

Methods

Apparatus

Stimuli were generated on a MacBook Pro using the Psychophysics Toolbox Extension (Brainard, 1997; Pelli, 1997) for MATLAB (Mathworks Systems) and presented on a Sony Trinitron GDM F520 Monitor (40 cm × 30 cm display size) at 1400 × 1050 pixels resolution. The screen was placed at a distance of 70 cm in front of the subjects in an otherwise fully darkened room, resulting in a pixel at the center of the screen extending for 1.4 minutes of arc. Eye position was measured using an Eyelink 1000 desktop system (SR Research, Mississauga, Ontario, Canada) utilizing an infrared camera and illumination. Stimuli consisted of the Brentano version of the Müller-Lyer-Illusion (see Figure 1) presented dark (40 cd/m²) on a bright background (80 cd/m²).

A bright background was used to eliminate the possibility of visual persistence due to slow decaying phosphor components. Persistence of the screen image would allow for visual integration of the figure across fixations.

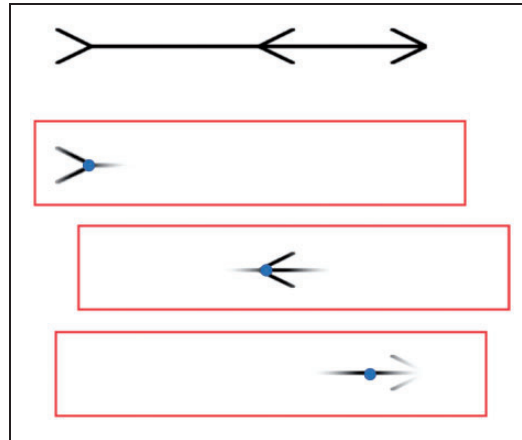


Figure 2. Shifting frame geometry. The top row shows the rightward pointing configuration of an entire Brentano stimulus. The bottom three rows show snapshots of the stimulus display based on this configuration for three different eye positions of the observer (from top to bottom: left, center, and right). Only a part of the stimulus inside a Gaussian window centered on fixation is revealed. Also shown is the fixation dependent shift of the reference frame (the red box) relative to the stimulus arrow (see paragraph 3 of Results for details). The small blue circles represent the POR (point of regard). For further explanation of the shifts in the box, see the text.

Stimulus Design

Each trial consisted of the sequential presentation of two Brentano stimuli, one of which was leftward-pointing and the other rightward-pointing (see Figure 1). One of these stimuli was displayed in the upper half of the screen and the other in the lower half of the screen. Which directional version of the stimulus was presented first, and whether the first stimulus was presented in the upper or lower half of the screen were randomized between trials. One of these stimuli, the *pedestal*, had an offset of the center arrow from the midpoint of the horizontal line. The other stimulus, the *test*, had the same pedestal offset and in addition a test offset. The test was equally likely to be the top or bottom figure, and thus equally likely to be first or second. To measure the strength of the Brentano bias, we manipulated the position of the middle point in these figures based on an asymmetry index. This index quantifies the offset from symmetry (the 50%/50% split point) in percent for the section of the figure delimited by pointed arrowheads (i.e., the left section of Figure 1(a) and the right section of Figure 1(b)). An asymmetry index of 0 therefore corresponds to a symmetrical arrangement, where the tip of the middle chevron cuts the length of the arrow base line exactly in half. A value of 5% corresponds to a 55%/45% split, with the pointed arrowhead section being longer.

The height of the stimuli as measured from the ends of the arrow wings was 1.87° (80 pixels). The stimulus width as measured from the tip of the arrow to the end of the tail was randomly chosen from the interval between 18.7° and 23.4° (800–1000 pixels) on each trial. The two stimuli within a single trial always had the same width. In some conditions, the stimuli were surrounded by a rectangular boundary box drawn in red. The dimensions of this box and the position of the stimulus were randomized as follows.

The horizontal and vertical positions of the stimuli on screen were randomly jittered trial by trial by up to 40 pixels independently in the horizontal and vertical directions. The width

of the margin between the Brentano figures and the reference frame on trials with a reference frame (see Figure 2) was randomly chosen from between 0.7° and 1.6° (30–70 pixels), independently for the top, bottom, left, and right margin. These randomizations ensured that the on-screen position of the middle chevron alone would not be a sufficient cue to the task in any of the conditions.

Trial Design

Each trial started with a fixation spot in the center of the screen. After gaze position remained within a circle of 2.3° (100 pixels) radius around the fixation spot for 300 milliseconds, the fixation target was extinguished and the first stimulus was drawn in its entirety in nonwindowed trials or within a Gaussian aperture window centered on fixation in aperture trials. If a reference frame was present in aperture trials, the frame was always drawn in its entirety and only the Brentano figure was subjected to the aperture windowing. The first stimulus remained viewable for 5 seconds.

In aperture trials, if the onset of a saccade was detected by the Eyelink system during that period, the stimulus display was immediately erased. The stimulus redrawn after the saccade ended with a new window at the new fixation position. Saccades were detected by a conjunction of a $30^\circ/\text{s}$ velocity threshold with a $8000^\circ/\text{sec}^2$ acceleration threshold and a 0.15° motion threshold.

After the 5 seconds had elapsed, the display automatically switched to the second stimulus of the trial, which was displayed in the same way as the first. The second stimulus also remained visible for a maximum of 5 seconds, or until the subject pressed a response key.

Subjects' responded by indicating whether the apex of the center arrow was nearer the midpoint of the horizontal line in the top or bottom figure.

Psychophysical Procedure

To reduce the possibility of expectation biases influencing the subjects' responses, we combined the 2AFC method with a roving pedestal (Morgan et al., 2013). The experimental design included three pedestal values and six probe values per pedestal. To determine pedestal values, subjects went through an initial setup phase for each condition where they adjusted the position of the middle chevron on the base arrow line using two computer keys until the stimulus appeared symmetrical. For each condition, this setting by method of adjustment was performed under viewing conditions identical to the trial presentation later during the experiment, that is, the reference frame and aperture window were applied. This setting was repeated three times. The three pedestal values then were fixed at the average of the three measurements and at 1% above and below that value. The probes for each pedestal were set at offsets of (-5% , -3% , -1% , 1% , 3% , 5%) relative to the respective pedestal value.

On each trial, it was randomly determined whether the first or second stimulus was drawn by using this trial's pedestal or probe value of the asymmetry index.

Model Functions

Response data from all trials, across all pedestals and probes, were fit with a two-parameter model. One of these parameters is the bias (μ) and the other is the internal noise (σ). These correspond to the P50 offset and the inverse slope of a single psychometric function in the MSS; however, here, we fit essentially three psychometric functions (precisely: three different one-dimensional cuts through a two-dimensional model function) with the same two

parameters. It was noted by Morgan, Grant, Melmoth, and Solomon (2015) that such functions can be computed by the use of doubly noncentral F-distributions. But evaluation of these distributions can be computationally expensive and produces only approximated results. In the Derivation of a Psychometric Model Function for 2AFC Roving Pedestal Experiments section, we provide the derivation of an alternate formulation of such model functions based on error functions that is much more economical to calculate. This derivation is based on the description in Patten and Clifford (2015). As the model function provides the probability of picking one of the stimuli based on the intensity of both, it is a two-dimensional probability function. For better visualization, we represent this function as a set of one-dimensional cuts through 2D stimulus space, resulting in one curve per pedestal value (see Figure 6).

Significance Testing

Model fitting was done through a maximum likelihood fit. For each set of parameters μ and σ , the likelihood of the data occurring under the model function associated with those parameters was computed by multiplying the model's predicted probabilities of the responses given across all trials. The model parameters were then chosen such that this overall likelihood of the data was maximized. We obtained confidence intervals for the model parameters by parametric bootstrapping. For this, subject responses for all trials were stochastically simulated using the best fit model function obtained in the previous step. The resulting simulated dataset was then maximum likelihood fit with a model function, and the resulting parameters were recorded. This was repeated 1000 times and the resulting parameter distributions for μ and σ were sorted by magnitude. The confidence interval for $p = .05$ was then obtained by finding the 0.025 and 0.975 quantile of the distribution (the 26th and 974th value in the ordered distribution).

Model Comparison

To test for statistically significant differences in model fit parameters between conditions, we carried out partial F-tests based on the likelihood ratio of the model fits as follows.

The two datasets in question were each individually fit with separate model functions (full model, four parameters). They were also fit with a model function using different parameters μ for the two conditions and a single parameter σ (reduced model for σ , three parameters), and with a model function using different parameters σ for the two conditions and a single parameter μ (reduced model for μ , three parameters). A log likelihood test was then used to determine the statistical significance of each parameter by comparing the logarithm of the likelihood ratio of the data under the full model and the data under either of the reduced models to a χ^2 -distribution with one degree of freedom (Wilks, 1938).

Subjects

We tested six subjects (three male, three female) with normal or corrected to normal vision, ranging in age from 28 to 74 years.

Comparison of Measurement Methods

To illustrate the influence of the experimental method on results obtained in measuring perceptual biases, we compared the biases obtained through method-of-adjustment to

those found through 2AFC and model fitting. As reported in the Methods section, at the beginning of each condition, we obtained three consecutive settings where subjects could adjust the middle point of the figure such that it appeared most symmetrical to them. During these settings, the same display method as during the 2AFC task was used, that is, stimuli were seen through aperture windows or static, with a static or eye position contingent reference frame.

The results of the comparison of these minute of angle (MOA) values to 2AFC bias estimates demonstrate a consistent overestimation of the bias through the method of adjustment settings (See Figure 7). The data points have been fit with a linear function. The slope of this function is one, indicating that both methods measure the same quantity at the same scale, but the vertical offset means that MOA results were consistently higher by 1.4 across all conditions. This result is presumably due to a changed criterion through the influence of cognitive strategies, though it should be pointed out that the tasks—set the stimulus to appear symmetrical for MOA, and pick the stimulus that looks more symmetrical for 2AFC—are ever so slightly different, as well.

This observation, however, underlines the need for methods that avoid cognitive biases in measuring perceptual effect and stresses the importance of method choice for the overall measurement results.

Results

Perceptual Bias

We first confirmed that our stimulus display indeed produces the perceptual bias commonly referred to as the Müller-Lyer “illusion.” To this end, we first used a static version of the stimulus display with no aperture window. Here, the entire double arrow stimulus was visible within the bounding box. For this condition, we found bias magnitudes ranging from 5.4% to 9.0% (Figure 3) well in agreement with the reported magnitude of the Müller-Lyer illusion (e.g., Segall, Campbell, & Herskovits, 1963).

This perceptual bias persisted when the stimulus was viewed through the gaze contingent aperture (Figure 4). Even though in this condition, subjects never saw more than one component of the figure at a time, their perception of the symmetry of the overall figure was still biased in the same direction as for the static version. The magnitude of the bias was slightly smaller for all six subjects compared with the static condition, but this difference was significant in only two of the subjects.

The existence of a bias in the perception of the global geometry of these stimuli under aperture viewing conditions suggests that the perceptual mechanisms giving rise to the bias must be operating on a representation that has been integrated across fixations. This integration requires the combination of visual stimulus fragments seen in each fixation with information about their relative position in the overall stimulus. This position information can either come from eye position signals based either in efference copy or proprioception, or from the visual neighborhood. To disambiguate these two possibilities, we manipulated the position of the box frame surrounding the double arrow stimulus in an eye position contingent manner such that the middle part of the arrow stimulus appeared displaced relative to the box in the direction of the perceptual illusion. This should have countered the bias toward seeing the middle arrow shifted away from the center of the box. To determine the shift of the box for fixations at other locations than the center arrow, a simple interpolation rule was applied. If fixation was at either end of the stimulus, no shift was applied. For fixations at other positions, the shift was ka/c , where k is the maximum shift, a is the distance of fixation from the center apex, and c is the distance of

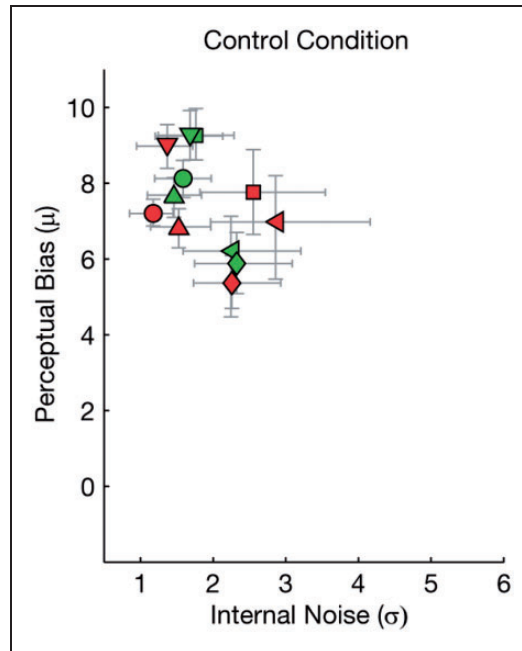


Figure 3. Perceptual bias and internal noise parameters for the control condition (static viewing with no gaze contingent aperture). Green symbols are for the condition with a static frame and red for the frame shift condition. Error bars for these result plots are 95% confidence intervals obtained from parametric bootstrapping.

the center apex from the end of the figure on the same side as fixation. Note that c is different on the two sides of the figure because the arrow is ingoing at one end and outgoing at the other.

In the light of the foregoing, the box-shifts shown in Figure 2 can be interpreted as follows. In the top row, fixation is at the end of the figure so the box is unshifted. In the middle row, fixation is on the apex of the middle arrow so the shift is maximal. In the bottom row, fixation is shifted inwards from the end of the figure so there is a small rightwards shift. Had fixation in the latter case been on the apex of the arrow, no shift would have been applied.

If stimulus integration were based on eye position information, this should not affect the perceptual bias at all, as the arrow stimulus itself was not changed by this manipulation. If, on the other hand, local visual reference is used to integrate individual aperture views of the stimulus, perception of the location of the central portion of the stimulus should be affected such that the measured size of the perceptual bias is reduced. If eye position were disregarded entirely in the stimulus integration process, this reduction in the size of the measured bias should correspond exactly to the size of the applied frame shift. In our manipulation, the shift had a magnitude of 5%, meaning that a symmetrically split stimulus would appear relative to the frame as having a 55%/45% split.

In Figure 5, we plot the perceptual bias versus the size of the applied frame shift separately for each of our six subjects. In two of our subjects (KS and KE), the reduction in bias was very close in magnitude to the applied frame shift; in the other four subjects, the reduction of bias was less than the visual shift of the frame box. For subject KS, we collected

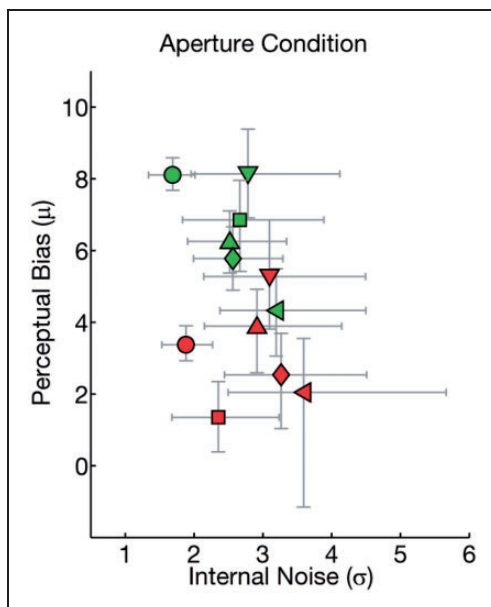


Figure 4. Perceptual bias and internal noise parameters for the aperture viewing condition. The magnitude of the perceptual bias is lower than in the static condition, and internal noise is somewhat increased, but the bias is qualitatively unaffected by aperture masking. Green symbols are for the static frame condition, and red symbols for the condition where the frame shifted in a gaze contingent manner.

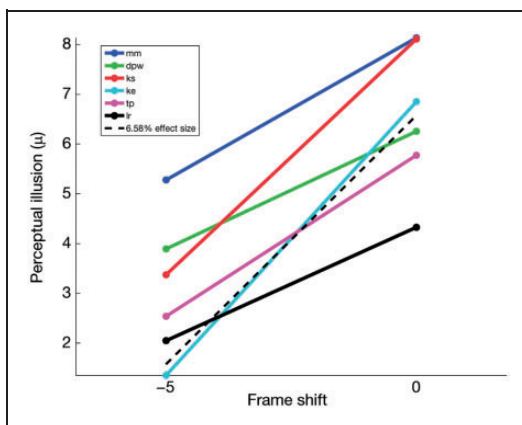


Figure 5. Perceptual bias plotted against frame shift. The dashed line represents the theoretical prediction if eye position is completely ignored at the average perceptual bias of all six subjects, 6.58.

an additional exploratory condition where the frame box was shifted by a magnitude of eight, corresponding to a 42%/58% split. This reduced the measured bias to 0.25, confirming the linear trend.

We also applied the shifting frame manipulation to the static control condition without an aperture viewing window. For static, nonwindowed stimuli, the manipulation of the reference frame position produced much smaller changes in the perceptual bias in three of

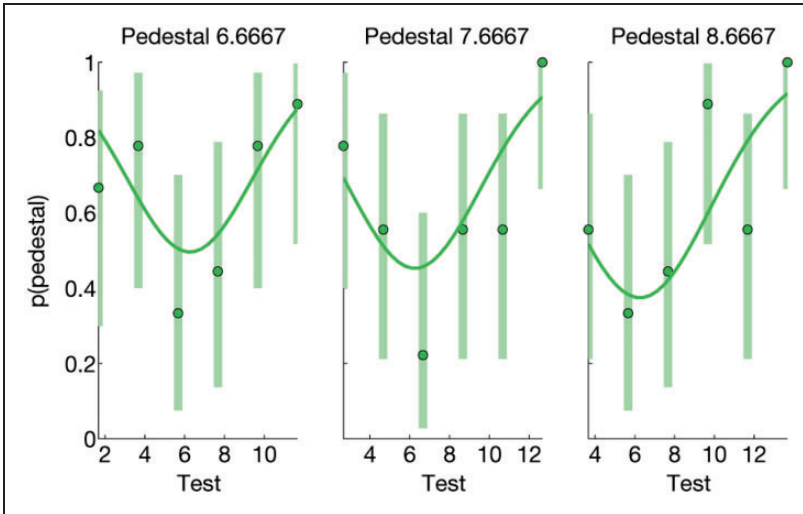


Figure 6. Example data and psychometric function for one of our subjects. Each panel represents a specific pedestal value, with the associated test values of each trial on the x-axis. On the y-axis is the probability that the subject chose the pedestal over the test as being closer to symmetrical. Each data point represents six repeats at the specific pair of pedestal and test, with the thin error bars representing the confidence interval based on a binomial distribution. The three green curves are parts of the max-likelihood best fitting psychometric function for this dataset. The fit parameters μ and σ determine the location of the central dip (μ) and the slope (σ) for all three curves.

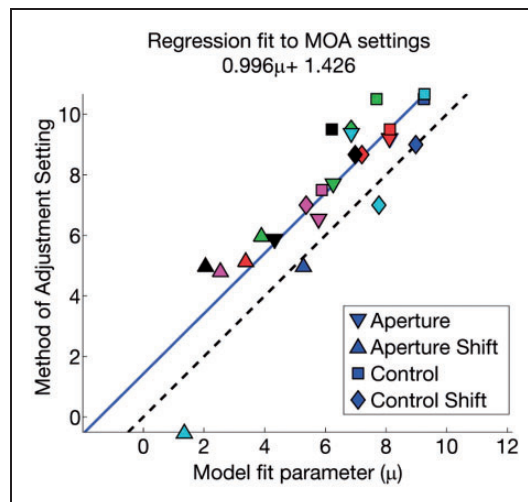


Figure 7. Comparison of model fit parameters and initial averaged method of adjustment settings across all subjects and conditions. The dashed line marks identity. The light blue line is a linear regression fit to all data points at $0.996 \times \mu + 1.426$.

Table 1. Test Statistics and Parameters for Pairwise Comparison Tests for Experimental (Base vs. Shift) and Control Conditions.

Subject	Aperture Window: Base vs. Shift				Static Control: Base vs. Shift			
	Base	Shift	χ^2	p	Base	Shift	χ^2	p
DPW	6.25	3.94	10.81	.001	7.68	6.86	5.09	.02
KE	6.90	1.37	15.70	$<10^{-4}$	9.27	7.81	5.31	.0212
KS	8.12	3.37	115.22	$<10^{-16}$	8.10	7.23	8.05	.0046
LR	4.30	2.17	4.77	.029	6.00	7.01	1.49	.2221
MM	8.14	5.29	7.91	.005	9.24	8.97	0.38	.5368
TP	5.79	2.62	17.61	$<10^{-4}$	5.88	5.37	0.91	.3388

Note. Bold cells are comparisons for which the associated chi-squared test indicated significant differences at the $p < .05$ level. All bias differences are highly significant in the aperture window condition. In the static control condition, only three subjects reach significance and the bias differences are much reduced in size.

our subjects and failed to produce any significant differences in the other three (see Table 1 for statistical details).

Discussion

Stable Bias With Aperture Synthesis

We found the perceptual bias present commonly reported for the Brentano figure essentially unaffected by our aperture window viewing condition, in which subjects could never see more than one of the three configurational elements of the stimulus figure concurrently. One method by which observers could do this is by building up a visual image over saccades resembling the extended image seen when they view the image as a whole. To do this accurately, they would have to store an icon of the part-view from fixation to fixation and take account of the changing positions of their gaze. We think this unlikely for three reasons. First, there is no other evidence that eye position can be sufficiently accurately registered, either by proprioception or by efference copy. Second, the evidence from “change blindness” and other experiments is that the visual image does not endure over fixations in an iconic form. Finally, we found that subject’s estimate of the midpoint of the figure was altered by manipulating the position of a surrounding frame between saccades. The results of this manipulation revealed that all of our six subjects had changed their perceptual bias, indicating that visual integration largely ignores eye position information and is dominated by visual context. In two of our subjects, the magnitude of the bias change was consistent with fully visual integration and discarded eye position information. While the magnitude of the bias in the other four subjects may indicate residual influence of eye position signals on the visual integration processes involved, we cannot exclude the possibility that the partially world-centric visual integration observed was due to external visual cues such as the screen boundary.

The alternative to a fully iconic and gaze-corrected representation is a mid-level representation of visual feature location. In fixations when the center arrow is revealed, subjects could note its position relative to the center of the frame. Suppose that this perceived position is biased by whatever process it is that produces the normal Muller-Lyer bias. Thus, a right-pointing arrow centered in the frame would appear shifted leftwards relative to a left-pointing arrow also centered in the frame. This information by

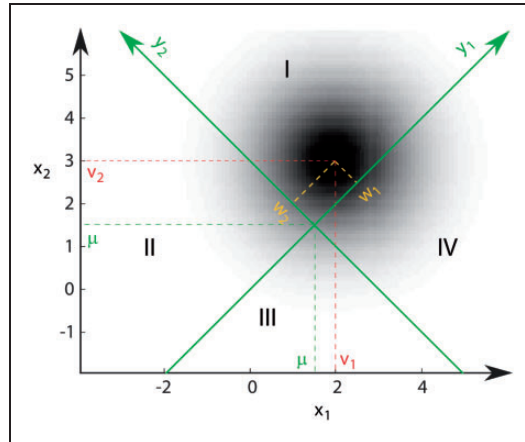


Figure 8. Probability of perceiving a pair of stimuli at intensities x_1 and x_2 for physical stimulus intensities $v_1 = 2$ and $v_2 = 3$. The green diagonal lines represent the decision boundaries for the task of judging the distance from the standard at $\mu = 1.5$. For points in quadrants I and III, the stimulus at v_1 appears closer to the standard, in quadrants II and IV, the stimulus at v_2 appears closer.

itself is not enough to compare the center arrow positions in the two stimuli, because there was a random shift of the stimulus within the frame from trial to trial, which was independent in the two stimuli. However, if the positions of all three arrow apices are noted relative to the surrounding box, the subject has exactly the same information that they have in any three-dot bisection task. The only manipulation that will defeat this computation is if the position of the box shifts between fixations, and we find indeed that we can manipulate the bias in this way.

We conclude that the relative visual location of features can be stored over saccades and that this allows the build-up of a spatially extended representation of space over saccades, although not in a fully iconic representation. Our account has much in common with the “landmark” theory of trans-saccadic localization advanced by Deubel (2004) and with the findings of Hayhoe et al. (1991).

Derivation of a Psychometric Model Function for 2AFC Roving Pedestal Experiments

In a true 2AFC experiment, each trial has two stimulus intensities associated with it. This adds complexity to the modeling step relative to standard psychophysics, because the underlying psychometric function then also needs to be two dimensional.

To derive its mathematical shape, we assume that perception of the two stimuli in each trial is subject to independent Gaussian noise of standard deviation σ . The probability for a pair of stimuli placed at physical intensities x_1 and x_2 to be perceived at intensities p_1 and p_2 is then a 2D Gaussian centered on (x_1, x_2) ; see Figure 8. Note that the two perceived stimuli have identical distance from the standard at μ along the two diagonal green lines. These decision lines therefore divide stimulus space into four response regions, with the percept of Stimulus 1 being closer to the standard in Regions I and III, and further away from it in Regions II and IV.

The probability of picking Stimulus 1 as closer to the standard is then the double integral of the probability distribution across regions I and III in Figure 3. Because the integration

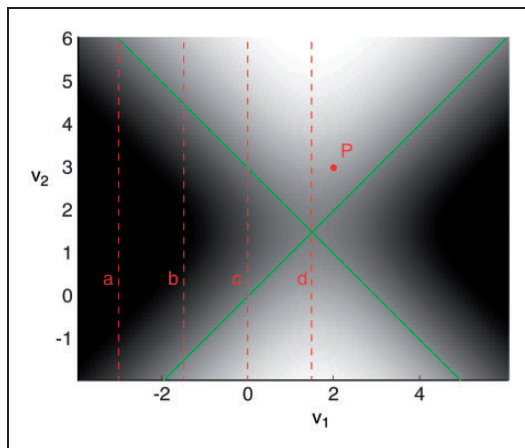


Figure 9. Psychometric function for $\mu = 1.5$, $\sigma = 1.25$. Shading at each point is determined by the probability of perceiving Stimulus 1 as being closer to the standard than Stimulus 2. Point P represents the example presented in Figure 3. The four red dashed lines represent pedestal values for sampling according to the roving pedestal method.

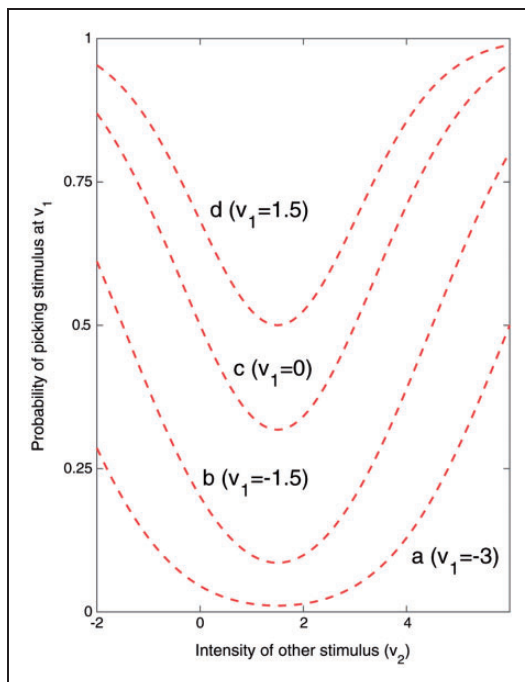


Figure 10. Four example slices of the psychometric function shown in Figure 9 corresponding to four different values for Stimulus 1. Note that these are different aspects of a single 2D psychometric function, not four separate functions.

limits in one of the dimensions depend on the other dimension, a closed form for the solution cannot be obtained in these coordinates.

But, based on the approach described by Patten and Clifford (2015), we can transform the problem into a rotated and shifted coordinate system, where the decision lines become coordinate axes and the reference point (μ, μ) becomes the origin.

Transformation into these new coordinates is achieved by

$$y_1 = \sqrt{2} \left(\frac{x_1 + x_2}{2} - \mu \right)$$

$$y_2 = \sqrt{2} \left(\frac{x_2 - x_1}{2} \right)$$

The probability distribution for perceiving a stimulus at location (y_1, y_2) in this new space is again a 2D Gaussian

$$p(y_1, y_2) = \frac{1}{2\sigma^2\pi} \exp\left(-\frac{(y_1 - w_1)^2}{2\sigma^2}\right) \exp\left(-\frac{(y_2 - w_2)^2}{2\sigma^2}\right)$$

where (w_1, w_2) are the physical stimulus intensities (v_1, v_2) in the transformed space.

The probability of perceiving the first stimulus as being closer to the standard in this new coordinate system is the integral of p over the first and third quadrants:

$$\psi = \int_0^{\infty} \int_0^{\infty} p(y_1, y_2) dy_1 dy_2 + \int_{-\infty}^0 \int_{-\infty}^0 p(y_1, y_2) dy_1 dy_2$$

Using the error function identity for the integral of the Gaussian and separating out the two dimensions, this becomes

$$\psi = \left[\frac{1}{2} - \frac{1}{2} \operatorname{erf}\left(-\frac{w_1}{\sigma\sqrt{2}}\right) \right] \left[\frac{1}{2} - \frac{1}{2} \operatorname{erf}\left(-\frac{w_2}{\sigma\sqrt{2}}\right) \right] + \left[\frac{1}{2} + \frac{1}{2} \operatorname{erf}\left(-\frac{w_1}{\sigma\sqrt{2}}\right) \right] \left[\frac{1}{2} + \frac{1}{2} \operatorname{erf}\left(-\frac{w_2}{\sigma\sqrt{2}}\right) \right]$$

which simplifies to

$$\psi = \frac{1}{2} + \frac{1}{2} \operatorname{erf}\left(-\frac{w_1}{\sigma\sqrt{2}}\right) \operatorname{erf}\left(-\frac{w_2}{\sigma\sqrt{2}}\right)$$

or in the original coordinates

$$\psi_{\mu, \sigma}(v_1, v_2) = \frac{1}{2} + \frac{1}{2} \operatorname{erf}\left(\frac{\mu - v_1 + v_2}{\sigma} - \frac{v_1 + v_2}{2\sigma}\right) \operatorname{erf}\left(\frac{v_1 - v_2}{2\sigma}\right)$$

This then is the psychometric function modeling the probability of perceiving a stimulus at v_1 as being closer to the standard at μ than a stimulus at v_2 , under perceptual noise of standard deviation σ .

An example function for $\mu = 1.5, \sigma = 1.25$ is depicted in Figures 9 and 10.

Declaration of Conflicting Interests

The author(s) declared no potential conflicts of interest with respect to the research, authorship, and/or publication of this article.

Funding

The author(s) disclosed receipt of the following financial support for the research, authorship, and/or publication of this article: Funding was received from the Leverhulme Trust, Grant RPG-20160-124.

References

- Brainard, D. H. (1997). The psychophysics toolbox. *Spatial Vision, 10*, 433–436.
- Day, R. H., & Duffy, F. M. (1988). Illusions of time and extent when the Müller-Lyer figure moves in an aperture. *Perception & Psychophysics, 44*, 205–210. doi:10.3758/BF03208042
- Deubel, H. (2004). Localisation of objects across saccades: Role of landmark objects. *Visual Cognition, 11*, 173–202.
- Hayhoe, M., Lachter, J., & Feldman, J. (1991). Integration of form across saccadic eye movements. *Perception, 20*, 393–402. doi:10.1068/p200393
- Mather, G., & Sharman, R. J. (2015). Decision-level adaptation in motion perception. *Royal Society Open Science, 2*, 150418. doi:10.1098/rsos.150418
- Morgan, M. (2014). A bias-free measure of retinotopic tilt adaptation. *Journal of Vision, 14*, 1–9. doi:10.1167/14.1.7
- Morgan, M. J., Findlay, J. M., & Watt, R. J. (1982). Aperture viewing: A review and a synthesis. *The Quarterly Journal of Experimental Psychology Section A, 34*, 211–233. doi:10.1080/14640748208400837
- Morgan, M. J., Grant, S., Melmoth, D., & Solomon, J. A. (2015). Tilted frames of reference have similar effects on the perception of gravitational vertical and the planning of vertical saccadic eye movements. *Experimental Brain Research, 233*, 2115–2125. doi:10.1007/s00221-015-4282-0
- Morgan, M. J., Melmoth, D., & Solomon, J. A. (2013). Linking hypotheses underlying class A and class B methods. *Visual Neuroscience, 30*, 197–206. doi:10.1017/S095252381300045X
- Patten, M. L., & Clifford, C. W. G. (2015). A bias-free measure of the tilt illusion. *Journal of Vision, 15*, 8. doi:10.1167/15.15.8
- Pelli, D. (1997). The videotoolbox software for visual psychophysics: Transforming numbers into movies. *Spatial Vision, 10*, 437–442.
- Plateau, J. A. F. (1836). Anorthoskop. *Bulletin de l'Academie de Bruxelles, 3*, 364.
- Rock, I., & Halper, F. (1969). Form perception without a retinal image. *The American Journal of Psychology, 82*, 425–440. doi:10.2307/1420438
- Segall, M. H., Campbell, D. T., & Herskovits, M. J. (1963). Cultural differences in the perception of geometric illusions. *Science, 139*, 769–771. doi:10.1126/science.139.3556.769
- Wilks, S. (1938). The large-sample distribution of the likelihood ratio for testing composite hypotheses. *The Annals of Mathematical Statistics*. Retrieved from <http://www.jstor.org/stable/2957648>
- Wright, M., Green, A., & Baker, S. (2000). Limitations for change detection in multiple gabor targets. *Visual Cognition, 7*, 237–252. doi:10.1080/135062800394784